

# Run-time Parameter Sensitivity Analysis Optimizations

Eduardo Scartezini<sup>1</sup>, Willian Barreiros Jr<sup>1</sup>., Tahsin Kurc<sup>2,3</sup>,

Jun Kong<sup>4</sup>, Alba C. M. A. Melo<sup>1</sup>, Joel Saltz<sup>2</sup>, and George Teodoro<sup>2,5</sup>,

<sup>1</sup>Department of Computer Science, University of Brasília, Brasília, DF, Brazil

<sup>2</sup>Department of Biomedical Informatics, Stony Brook University, Stony Brook, NY, USA

<sup>3</sup>Scientific Data Group, Oak Ridge National Laboratory, Oak Ridge, TN, USA

<sup>4</sup>Biomedical Informatics Department, Emory University, Atlanta, GA, USA

<sup>5</sup>Department of Computer Science, Universidade Federal de Minas Gerais, Belo Horizonte, MG, Brazil

wbarreiros@aluno.unb.br, {albamm}@unb.br, jun.kong@emory.edu, {tahsin.kurc, joel.saltz}@stonybrook.edu, george@dcc.ufmg.br

**Abstract**—Efficient execution of parameter sensitivity analysis (SA) is critical to allow for its routinely use. The pathology image processing application investigated in this work processes high-resolution whole-slide cancer tissue images from large datasets to characterize and classify the disease. However, the application is parameterized and changes in parameter values may significantly affect its results. Thus, understanding the impact of parameters to the output using SA is important to draw reliable scientific conclusions. The execution of the application is rather compute intensive, and a SA requires it to process the input data multiple times as parameter values are systematically varied. Optimizing this process is then important to allow for SA to be executed with large datasets. In this work, we employ a distributed computing system with novel computation reuse optimizations to accelerate SA. The new computation reuse strategy can maximize reuse even with limited memory availability where previous approaches would not be able to fully take advantage of reuse. The proposed solution was evaluated on an environment with 256 nodes (7168 CPU-cores) attaining a parallel efficiency of over 92%, and improving the previous reuse strategies in up to 2.8×.

**Keywords**—Microscopy Imaging; Sensitivity Studies; Memory-Aware Scheduling.

## I. INTRODUCTION

The process of quantifying the impact of the input parameters of an application workflow on its outputs is defined as sensitivity analysis (SA) [1]. This analysis is carried out by re-executing the target application and quantifying the output results changes as parameters' values are modified. The use of SA methods is important as it can (i) improve our understanding on the correlation between workflows' inputs and outputs, (ii) improve the quality/stability of the application workflow output by identifying sources of uncertainty, and (iii) simplify workflows by either fixing parameters or removing parts with little impact on the output.

The pathology image analysis domain that motivates this work may benefit from SA. A typical application in this area processes whole-slide tissue images (WSI) that may have in the order of 120K×120K pixels or 50GB in size through a series of transformations that include normalization, segmentation, feature computations, and other correlative analysis. The first three stages are more compute intensive and output

segmented objects (e.g., cells' nuclei) along with their shape and texture data features. This information may be used in several ways, for instance, to perform survival correlations. Our motivating application workflow is presented in Figure 1, which shows the main computing stages and their internal workflow of tasks.

Much work has been done to adapt and employ SA methods for other domains [2], [3], [4], [5]. Nevertheless, the use of SA in practice can be challenging given that the many applications are very compute demanding. This is the case in pathology image analysis, where the execution of a single WSI can take hours when processed in a node. This is worsen by the fact that an analysis study will employ hundreds of WSIs and our application has several parameters (Table I). Thus, processing all images as parameters are changed in a SA is a very costly process, which motivates this work.

Table I: Application parameters and their range values [6].

Parameter	Description	Range Values
B/G/R	Background detection thresholds	[210, 220, ..., 240]
T1/T2	Red blood cell thresholds	[2.5, 3.0, ..., 7.5]
G1/G2	Thresholds to identify candidate nuclei	[5, 10, ..., 80]
MinSize(minS)	Candidate nuclei area threshold	[2, 4, ..., 40]
MaxSize(maxS)	Candidate nuclei area threshold	[900, ..., 1500]
MinSizePl (minSPL)	Area threshold before watershed	[5, 10, ..., 80]
MinSizeSeg (maxSS)	Area threshold in final output	[2, 4, ..., 40]
MaxSizeSeg (minSS)	Area threshold in final output	[900, ..., 1500]
FillHoles(FH)	propagation neighborhood	[4-conn, 8-conn]
MorphRecon(RC)	propagation neighborhood	[4-conn, 8-conn]
Watershed(WConn)	propagation neighborhood	[4-conn, 8-conn]

In a previous work, computation reuse has been evaluated as an optimization to speedup SA [6], [7]. Computation reuse opportunities occur in SA studies because the same dataset is processed multiple times as parameters sets are systematically varied. These parameter sets may have subsets of parameters with the same values, which allows for parts of the application workflow to be reused. In our example application (Figure 1), there is opportunity for reuse either of entire stage instances (coarse-grain) stages when parameters used by instances are the same, or among a

subset of the internal tasks (fine-grain) when only a parts of the parameters are equal. A previous work [6] has proposed a strategy called Reuse-Tree Merging Algorithm (RTMA) that may take advantage of reuse in both granularities. However, its reuse capabilities are limited because the memory required by a stage to executed increases proportionally with the computation reuse employed. This problem is worsened in target systems with moderate to small per CPU-core memory availability and/or when the input data is large.

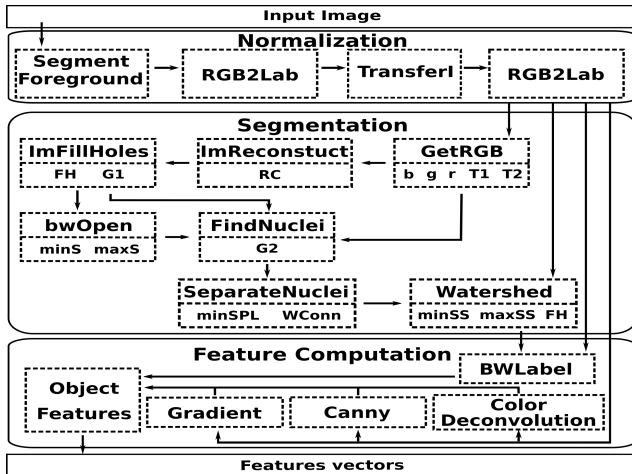


Figure 1: Motivating application stages: normalization, segmentation and feature computation stages. Operations used in each stage and parameters are shown with parameters.

In order to address such problems, we proposed a new reuse approach called Runtime Memory-Efficient Scheduler for Reuse (RMSR) that combines an off-line analysis with an on-line scheduler to orchestrate the execution and maximize reuse by removing the memory limitation aspect of RTMA. As a consequence, RMSR improved RTMA in up to  $2.8\times$  in our experimental analysis. We have also executed large-scale runs on a distributed memory machine with 256 nodes (7,168 CPU cores) in which a parallel efficiency of about 0.92 was attained. This demonstrates that the gains with the proposed optimizations are maintained in large-scale SA runs. This level of performance improvement opens new opportunities for using SA in our application domain.

The rest of this paper is organized as follows: Section II describes the Region Templates Framework (RTF) in which the proposed optimization was build. RMSR is presented in Section III, and experimental evaluation is detailed in Section IV. Further, Sections V and VI discuss, respectively, the related work and conclusions.

## II. REGION TEMPLATES FRAMEWORK

The Region Templates Framework (RTF) was developed to enable the execution of dataflow applications on large scale distributed environments [8]. The main domains of the RTF include data-intensive applications that use data elements represented in low dimensional spaces (1D, 2D

or 3D) with an optional temporal component. Examples of these applications include medical image segmentation and object annotation [9].

The RTF is comprised by the data abstraction model, the hierarchical storage layer, and the runtime system. The data abstraction defines data object structures that are commonly used. These objects are managed by the hierarchical storage that saves and retrieves them in a distributed memory machine. The storage is optimized by using multiple memory layers, such as RAM, SSD, HDD etc, that can be local and/or distributed in a set of nodes.

The runtime system of the RTF allows for the application to be represented and executed as hierarchical workflows, comprised of coarse-grain stages in which each stage can be a workflow of fine-grain tasks. The execution on a distributed memory machine follows a Manager-Worker model and stage instances are assigned for execution with Workers in a demand-driven fashion. As such, the fine-grain tasks that implement a given stage instance are executed within a single Worker. Further, a Worker may use all computing resource available in a node (CPU cores, GPUs, etc) by dispatching tasks in multiple devices concurrently [10], [11], [12], [13].

In the RTF, application stages communicate by writing/reading data objects from the hierarchical storage. This feature (i) alleviates the application development effort as inter-node communication is managed by the runtime; and, (ii) also allows for the system to automatically perform decisions about the data and execution placements with the goal, for instance, of minimizing data movements.

### A. Executing Sensitivity Analysis (SA) in the RTF

This section describes the components built on top of the RTF for executing SA (Figure 2). A SA study receives the input data, application workflow, and parameters to be analyzed. It then executes a SA method that will select parameters' values sets for which the application should be executed. Those parameters sets and application workflow are analyzed for computation reuse, and the resulting workflow is dispatched for execution with the RTF in a high-performance machine. The result of this execution is a metric of difference (e.g., Dice or Jaccard) that measures the difference between application results (segmentation) for each parameter set vs. segmentation results computed using the application default parameters. These metric values are returned to the SA module that computes indices with the importance of each parameter to changes in the output.

SA can be computed through a number of methods. Some include screening methods as the Morris One-At-A-Time (MOAT) [2], which are commonly employed to efficiently identify non-important parameters. Further, we can also employ other more comprehensive methods that calculate importance measures, such as Pearson's and Spearman's

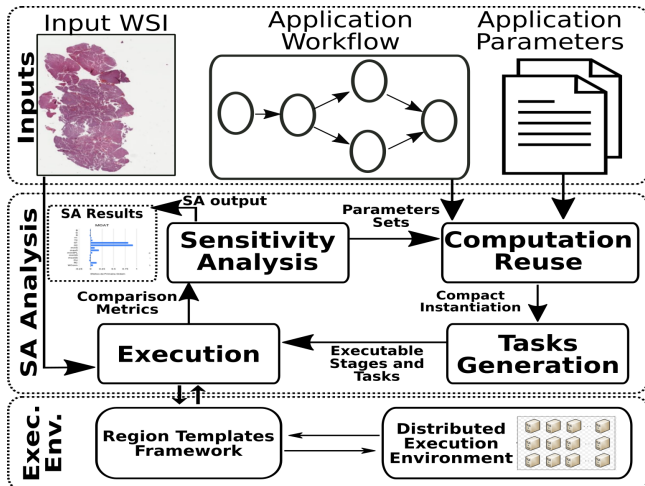


Figure 2: Architecture of the overall SA framework.

correlation coefficients [1] or the Variance-based Decomposition (VBD) [3]. These methods were listed according to their demands in the number of application runs (sampling size), and they are typically used in coordination. For instance, MOAT can be employed first to reduce the parameters to a core set of known important ones, before other costly methods are executed. The methods may use different approaches to select the parameters sets to be evaluated: Monte Carlo sampling, Latin hypercube sampling (LHS) [14], quasi-Monte Carlo sampling with Halton or Hammersley sequences, etc.

### B. Multi-level Computation Reuse

The RTF used in this work performs the execution using hierarchical workflows with two levels: stages and tasks. This raises possibilities for reuse of stages (coarse-grain) and tasks (fine-grain). In stage-level reuse the sets of parameters' values for a given stage are compared to find stages that use exactly the same input parameters. In that case, a single copy of a duplicate stage is instantiated and dependencies in the workflow are fixed so that downstream stages can receive the information. Figure 3 presents an example of an application workflow and parameters sets to execute in a SA. Further, it depicts the application instantiation in the replica-based with no reuse and the compact composition in which replicated stages are not executed multiple times.

Stage-level reuse can not take advantage of partial reuse among stages. For that sake, task-level reuse has been proposed [6]. The task-level reuse will merge together stage instances with overlapping (but not equal) set of parameter values. The replicated tasks from the merged stage instances are then removed, and the remaining ones will be part of a single, coarser-grain, stage instance. This creates an additional challenging with respect to the number of stages that can be merged. As the number of stages merged increases, the amount of memory required to executed that stage also grows. A previous work has implemented an algorithm

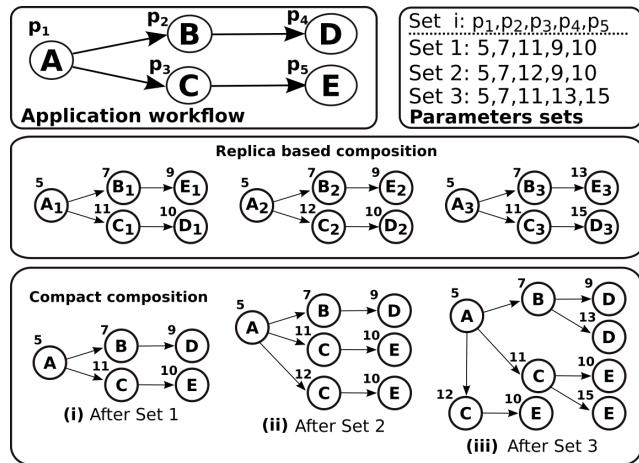


Figure 3: Example of a workflow composition. This composition can be performed by either fully replicating the base workflow for each parameters set, or performing a compact composition, which excludes the execution of repeated tasks.

called Reuse-Tree Merging Algorithm (RTMA) [6] in which the maximum number of stages (MaxBucketSize) to be merged is fixed and selected by the user.

The RTMA organizes the stage's tasks in a tree structure where each task is a node, as illustrated in Figure 4. This example uses a stage workflow with three tasks. Stages are assigned to different branches of the tree according to the parameters' values used by their internal tasks. After the tree is built, the deeper the first common ancestor is for a pair of stages instances, the higher the amount of reuse among them. Due to the limit in the number of stages that can be merged, RTMA generates buckets of stage instances to be merged respecting the MaxBucketSize value.

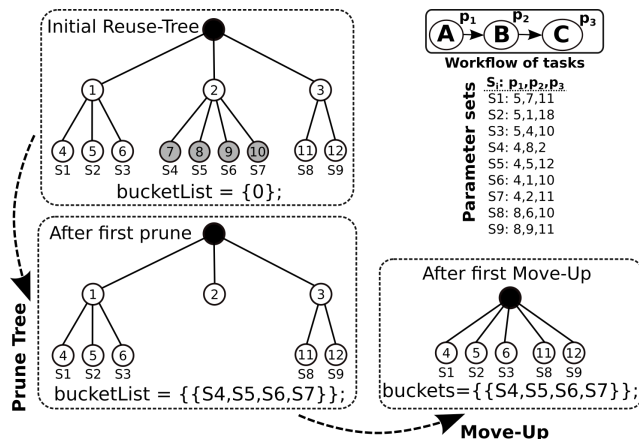


Figure 4: RTMA example with 12 stage instances that are grouped in buckets of MaxBucketSize=4.

The merging or choice of these buckets of stage instances is an iterative process. The algorithm searches for MaxBucketSize stages with the same parent in the tree that to fill a bucket, creates a bucket for those stages,

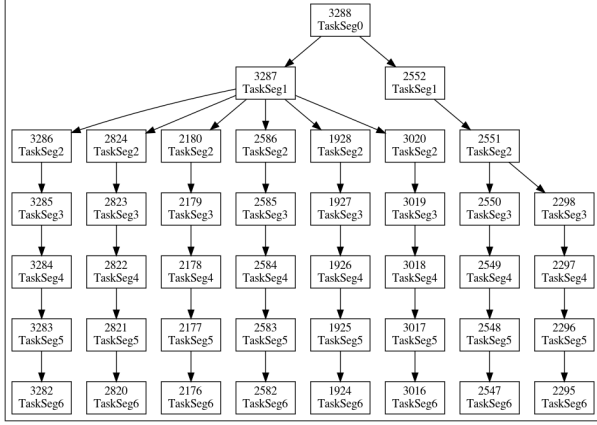


Figure 5: Typical workflow with 7 tasks (Seg0,...,Seg6) after passing a computation reuse analysis with a  $\text{MaxBucketSize}$  of 8: the resulting tasks tree of the merged stage has a width and the memory demands proportional to  $\text{MaxBucketSize}$ .

and removes them from the tree. This is computed for all leaf nodes and corresponds to the prune phase of the algorithm. Further, the remaining leaf nodes (stage instances not assigned to a bucket) are moved one level up in the tree, and the same process is repeated until all stage instances are assigned to a bucket. An example of these operations for  $\text{MaxBucketSize}=4$  is presented in Figure 4. Stages S4-S7 have the same parent and are sufficient to fill a bucket, so they are removed from the tree. Since other leaf nodes with a common parent are not sufficient to create more buckets, the algorithm will go to the move-up phase. Nodes 4-6 are moved to the parent node of their parents, as are nodes 11 and 12. These leaf nodes' parents are removed from the tree along with any other childless node (e.g., node 2). Finally, the new tree can have the same process re-executed until all stages are not assigned to a bucket.

### III. RUNTIME MEMORY-EFFICIENT SCHEDULER FOR REUSE(RMSR)

The main purpose of the RMSR algorithm is to address the suboptimal gains with reuse in RTMA due to its limited merging ( $\text{MaxBucketSize}$ ). A merged stage in RTMA will have a typical form of a tree (Figure 5), where the tree width is proportional to  $\text{MaxBucketSize}$ . Because the memory is limited, the number of stages that can be merged ( $\text{MaxBucketSize}$ ) must be adjusted according. One could think of using a disk storage as an auxiliary memory to allow for larger  $\text{MaxBucketSize}$  and improve reuse. However, this is prohibitive in our use case application because the tasks are rather fine-grain and storing results outputted by all tasks (large images) in each stage is more costly than the execution time of the tasks.

The main idea of the RMSR is to modify the order in

which tasks within a coarse-grain stage are executed to decouple the  $\text{MaxBucketSize}$  from the memory actually used to execute the application. It works as an additional run-time phase to RTMA that receives a set of merged stages and limits the number of branches of the task tree (Figure 5) that are being executed/active at any time in the execution. This is done by allowing only a parameterized number of paths (activePaths) from the root to the leafs of the tree of tasks representing a stage to be concurrently active. For each of the active paths executed by RMSR, the tasks in that subtree are processed in a depth-first order, which limits the number of processing paths active (and using memory) regardless of the  $\text{MaxBucketSize}$  employed to build that stage. As a consequence, arbitrary high  $\text{MaxBucketSize}$  values can be used to merge stages as long as the activePaths are controlled during the execute to limit memory utilization.

---

#### Algorithm 1 RMSR tasks scheduler

---

```

1: Input: stageTaskTree, activePaths
2: taskStack  $\leftarrow$  stageTaskTree.root
3: while taskStack  $\neq$   $\emptyset$  or stageTaskTree  $\neq$   $\emptyset$  do
4:   if taskStack  $\neq$   $\emptyset$  and activePaths  $>$  0 then
5:     activePaths  $-$   $-$ 
6:     task  $\leftarrow$  taskStack.pop()
7:     task.run()
8:      $\triangleright$  Resolve deps/insert new tasks in the stack
9:     for all dep  $\in$  task.dependents do
10:      dep.nDependencies  $-$   $-$ 
11:      if dep.nDependencies  $==$  0 then
12:        taskStack.push(dep)
13:        stageTaskTree.remove(dep)
14:     activePaths  $+$   $+$ 

```

---

The Algorithm 1 describes the main steps of the depth-first style execution of a stage workflow of tasks. It receives as input the stage tree of tasks and the number of active paths to use. The main loop from lines 3-14 will execute until all tasks have been processed. It will then check whether there are tasks available for execution (*taskStack* not empty) and the maximum number of active paths was not reached. If both are true, a new task is selected for execution from the top of the *taskStack* to assert a depth order. The task is executed (line 7) and tasks that depend on it are pushed to the *taskStack* once they have all dependencies resolved.

Although Algorithm 1 is presented in a sequential fashion, it is executed by multiple threads in a Worker to select the next task to process. Each thread will deal with a path per time. Also, we want to highlight that the algorithm developed was designed for applications with tasks that are homogeneous in terms of memory demands. For heterogeneous cases, RMSR would have to limit the number of active paths to that of the memory spent by the most demanding tasks, which would be suboptimal.

-real

#### IV. EXPERIMENTAL EVALUATION

The experiments were executed using brain tissue images from cancer studies [9]. The application used in our evaluation consists of the normalization, segmentation and comparison stages (see Figure 1). The comparison metric implemented is the Dice coefficient of objects found for each parameter set used in the SA vs. those generated using the application default parameters. The experiments were executed on a cluster machine on which each node had a dual socket Intel Haswell (E5-2695 v3) CPUs (14 cores each CPU), 32 GB of memory, and Red Hat Linux. The machines are inter-connected with Infiniband switches, and codes were compiled with Intel Compiler 13.1 using “-O3”. All execution times refer to the application makespan, including I/O, scheduling, and actual processing times.

##### A. The Impact of Computation Reuse to Performance

This section presents the impact of performing computation reuse for SA runs. In this setting, we have used a MOAT study with a two parameter sampling sizes (number of application runs) created using a quasi-Monte Carlo with a Halton sequence. We have compared the execution without reuse (No reuse), with reuse at the Stage Level only, and with reuse at task level that employs the RTMA proposed in the previous work.

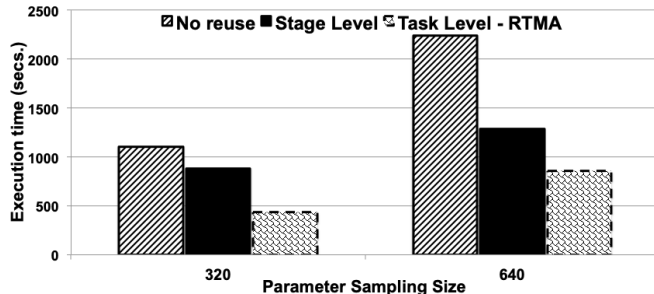


Figure 6: The performance benefits of different computation reuse strategies.

The experimental results are presented in Figure 6. As shown, the gains with reuse of computation are significant for both strategies and parameter sample sizes. In the case with 640 parameter sets, the Stage Level reuse attained a speedup of about  $1.7\times$  as compared to not reusing computation (No reuse). Further, the use of the task level reuse with RTMA (multi-level reuse) resulted in gains of  $2.6\times$  and  $1.5\times$ , respectively, on top of the No reuse and Stage Level approaches. The experiment also shows that gains with the reuse are higher with a larger parameter sampling size, which was expected due to the higher probability of duplicate computations in coarse (large images)-/fine-grain cases. While this section demonstrates that the performance benefits with computation reuse can be very significant, the

actual performance attained by the RTMA is limited by number of stages it can merge together (MaxBucketSize). In the next section we compare the performance of RMSR designed to deal with the memory limitations to RTMA.

##### B. The Impact of the Memory Availability to Computation Reuse (RMSR vs RTMA)

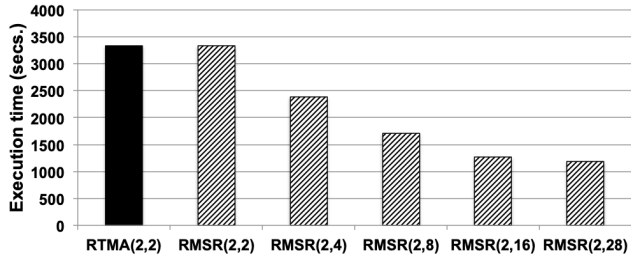
This section compares the performance of RMSR to RTMA [6]. It is performed under scenarios with different memory availability, which is the main aspect affecting the RTMA performance. Also, we use a MOAT SA study with 800 parameter sets and input images with  $4K\times 4K$  pixels.

To limit the algorithms memory utilization, we have varied their parameters with respect to bucket size and active paths used. The algorithms configurations are defined as  $RTMA(Y,X)$  and  $RMSR(Y,X)$ , where Y corresponds to the internal parallelism (number of threads used in a Worker) and active paths in the case of RMSR. The X parameter is the MaxBucketSize used. It is worth recalling that RMSR is able to increase the X value while limiting the memory utilization with the number of active paths. Each experiment employs a fixed Y value in RTMA and RMSR to isolate the parallelism gains and focus on the computation reuse. The Y or internal parallelism used is equals to the X employed in RTMA.

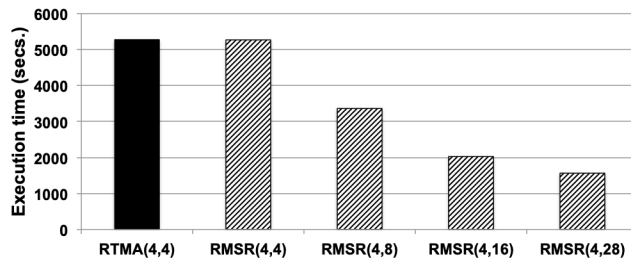
To setup the maximum memory used in each experiment we used the minimum reuse case (RTMA with MaxBucketSize of 2) as a baseline (6 GB), and have doubled the memory availability until the RTMA execution fits into the 32 GB available in our target machine. This results in the configurations with 6 GB, 12 GB, and 24 GB as presented in Figure 7. First, for all memory configurations, the performance differences of RTMA and RMSR are negligible when the same Y and X values are used. This indicates that the RMSR scheduling costs are not significant. Further, when X (or MaxBucketSize) is increased for RMSR while keeping Y (active paths and threads) the same as that used by RTMA, the RMSR performance is improved. For instance, for (large images) the case with 6 GB of memory (Figure 7a)  $RMSR(2,28)$  is  $2.8\times$  faster than  $RTMA(2,2)$ . This performance gain tends to decrease when the memory availability is higher, because RTMA can perform more reuse. However, the RMSR gains are still significant in the case with 24 GB of memory, since the  $RMSR(8,28)$  is  $1.6\times$  faster than  $RTMA(8,8)$ . In all cases, the gains are a result of the RMSR ability to perform more aggressive merging (or computation reuse) while restricting the memory utilization during the execution.

##### C. Impact of the Input Data Size to the Computation Reuse (RTMA vs RMSR)

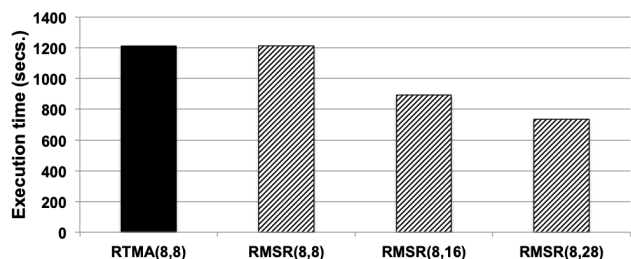
The input data size is another aspect that affects the computation reuse in RTMA. As the data size used grows, the application workflow demands more memory for execution,



(a) RTMA(2,2) or no reuse vs. RMSR with varying bucket size - Memory availability of 6 GB.



(b) RTMA(4,4) vs. RMSR with varying bucket size - Memory availability of 12 GB.



(c) RTMA(8,8) vs. RMSR with varying bucket size - Memory availability of 24 GB.

Figure 7: Comparison of the RTMA and RMSR in settings with different memory availability. While the RTMA has to maintain a fixed upper bound for the computation reuse stage merging (MaxBucketSize) for each memory configuration, the RMSR is able to increase the merging size a control the memory use through the execution.

which results in the need of using smaller MaxBucketSizes in RTMA. In this section, we quantify the amount of task reuse that RTMA and RMSR can achieve when processing larger images (9K×9K, 10K×10K, and 11K×11K pixels). We want to highlight that these image sizes are a common case in our domain, because current microscopes can generate images with resolutions in the order of 120K×120K pixels. For that sake, we have measured the maximum bucket size (MaxBucketSize) that RTMA would be able to use for potential target machines with larger memory: 64 GB and 128 GB. Then, we computed the task reuse that RTMA and RMSR would be able to perform for a VBD SA study with 8,000 parameter sets (runs).

The results are presented in Table II, where BucketSize

Table II: Reuse attained by RTMA and RMSR for different image sizes and two potential target machines with 64 GB and 128 GB of memory.

	Image Size	Machine with 64 GB		Machine with 128 GB	
		BucketSize	Reuse	BucketSize	Reuse
RTMA	9K×9K	4	31.75%	8	36.32%
	10K×10K	3	27.73%	6	33.57%
	11K×11K	2	21.82%	5	27.94%
RMSR	9K,10K,11K	10	36.36%	10	36.36%

refers to the MaxBucketSize that could be employed in RTMA for each pair image size and memory available. The RMSR used a BucketSize of 10 that leads to reuse close to maximum in this particular parameter set. As may be noticed, even with machines with large memory sizes, the reuse with RTMA would be significantly reduced with the use of big images, whereas using RMSR would preserve such performance gains. For instance, for the case with 64 GB and images with 11K×11K, RMSR would be able to reuse about  $1.6\times$  more tasks than RTMA.

#### D. Multi-core and Multi-node Scalability

Finally, in this section, we evaluate the scalability of the execution with RMSR in a multi-core and distributed memory environment. Figure 8a shows that the application attains good speedups as the number of computing cores increases. However, the speedups are slightly smaller than the ideal speedup, which is expected in this case because the memory and overall I/O subsystems are shared by the CPU cores (threads).

Further, we executed the application on a multi-node setting with a larger imaging dataset of 6,113 4K×4K brain tissue image tiles. The purpose of this experiment is to evaluate the overall performance of our system and optimizations on large-scale experiments. The execution times are presented in Figure 8. As shown, the execution scaled well as the number of machines used increases and it attained an parallel efficiency of about 92% for the configuration with 256 nodes. This demonstrates that the gains with our optimizations are maintained in large-scale runs.

#### V. RELATED WORK

Computation reuse has been extensively employed in multiple application domains [2], [15], [16], [17], [18], [19], [20]. It can be categorized according to the reuse granularity (fine-grain, coarse-grain or both), the reuse strategy (memoization or analytic), and whether the implementation requires customized hardware. Fine-grain reuse can lead to more reuse opportunities, but may also be more complex to exploit due to inherent overheads. Also, the memoization that uses caches in an attempt to attain reuse is more popular. However, it is inefficient in data-intensive applications due to the high caching amounts that would be necessary. In this case, an analytic approach can be used to compute

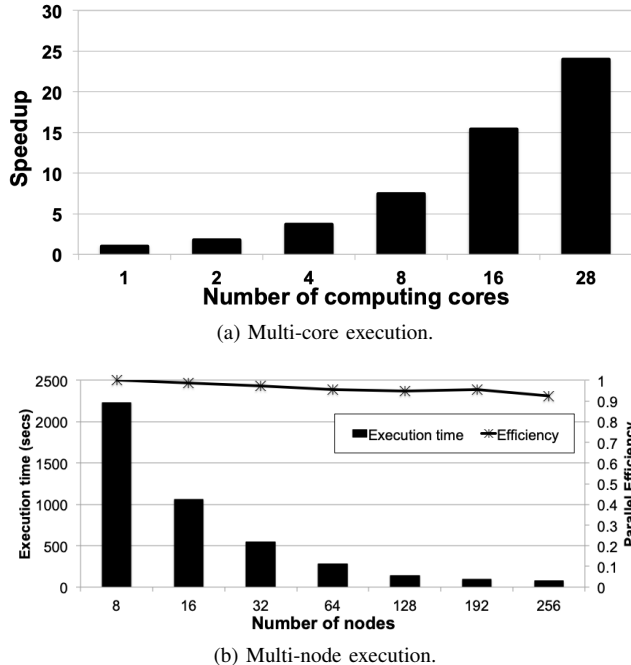


Figure 8: Execution scalability of our system in large-scale SA.

reuse opportunities in an application and link the output of operations to the locations in which it is to be reused, alleviating the caching pressure.

Other works employed reuse buffers to retrieve low-level instructions sub-results [15]. Their solution either ends instruction pipelines earlier, reducing resources conflicts, or breaks next instructions dependencies through reuse, thus reducing the overall execution cost. Another strategy on hardware [21] has implemented an interesting reuse approach with the goal of minimizing power consumption. In this case, they would profile the application to quantify reuse regions, whose granularities were chosen taking into account the benefits.

Computation reuse in distributed environments has been employed by caching secure-function evaluation (SFE) that are used by multiple clients in a server-client scheme [16]. As one may notice, this strategy would require a coarse-grain task reuse for attaining scalability. Computation reuse has also been employed in bioinformatics [17], [18]. In [17] outputs from full application runs are stored and reused, whereas [18] utilizes memoization to save partial results in the process of comparing proteins.

More recently Riera et al. [19] proposed using fine-grain reuse on deep neural networks as a way to reduce energy consumption. They leveraged the fact that such networks are tolerant to small precision variations, which increases the amount of reuse opportunities. This concept was implemented on hardware-level, but even if used as

an analytic method on software-level, its reliance on error-tolerant applications makes it not applicable to the domain discussed in this work. Another recent work by Li Liam et al. [20] has performed computation reuse in application tuning. Their work represents the application as a directed acyclic graph in which coarse-grain stages can be reused. Reuse is attained at runtime by finding pre-computed results. Still, the use of only coarse-grain task with a memoization strategy limits its use with applications that deal with small-scale datasets.

While there is a large number of works on computation reuse, we have not been able to find a work that would lead to efficient reuse in our domain. Our application is very compute intensive and manipulates large images, as such, requires execution on high-performance distributed memory machines. The large datasets used and processed are a limitation for using memoization, which is employed in most of the literature. To overcome this limitation we developed a novel analytic approach to identify reuse in the application workflow. Also, we have not seen multi-level reuse in other works in the literature, neither have we found approaches that leverage run-time scheduling to reduce the memory utilization with the goal of improving reuse.

## VI. CONCLUSIONS

Sensitivity analysis is an important tool employed on several domains, which has its use in practice limited in pathology image analysis because of the high computation costs involved. The computation reuse is one of the potential optimizations that may reduce SA costs. A previous work [6] has developed RTMA for that sake. However, the reuse capabilities of RTMA are limited by the memory available in the target machine, which would significantly reduce the optimization opportunities in several scenarios. To overcome this limitation, we proposed and implemented RMSR in this work. RMSR allows for aggressive computation reuse without increasing the memory demands as in the case of RTMA. As a consequence, RMSR has been able to improve the performance of RTMA in up to about  $2.8\times$ . Further, we have also shown that the gains of RMSR were maintained in large-scale runs in which a parallel efficiency of about 0.92 was attained in a distribute memory machine with 256 nodes. This level of performance should allow SA to be more widely use in the pathology image analysis.

As a future work, we intend to evaluate other optimizations to improve the performance in computation reuse. For instance, we want to analyze the impact of automatically adjusting the tasks granularity with the goal of maximizing reuse. It will be interesting to see the impact of the workflow generated in that case with respect to the tasks granularity and the potential effects in scheduling overheads, for instance, if tasks are too fine-grained. We also argue that a single workflow generation is suboptimal, and that the best approach would also consider the input set of

parameters to be evaluate with the application. In this case, the application execution graph can be enriched with the actual reuse information derived from parameters.

**Acknowledgments.** This work was supported in part by 1U24CA180924-01A1 from the NCI, R01LM011119-01 and R01LM009239 from the NLM, CNPq, Capes/Brazil grant PROCAD-183794, and NIH K25CA181503. This research used resources of the XSEDE Science Gateways program under grant TG-ASC130023.

## REFERENCES

- [1] A. Saltelli, S. Tarantola, F. Campolongo, and M. Ratto, *Sensitivity Analysis in Practice: A Guide to Assessing Scientific Models*. Wiley, 2004.
- [2] M. D. Morris, "Factorial sampling plans for preliminary computational experiments," *Technometrics*, vol. 33, no. 2, pp. 161–174, 1991.
- [3] V. G. Weirs, J. R. Kamm, L. P. Swiler, S. Tarantola, M. Ratto, B. M. Adams, W. J. Rider, and M. S. Eldred, "Sensitivity analysis techniques applied to a system of hyperbolic conservation laws," *Reliability Engineering & System Safety*, vol. 107, pp. 157 – 170, 2012.
- [4] F. Campolongo, J. Cariboni, and A. Saltelli, "An effective screening design for sensitivity analysis of large models," *Environmental Modelling & Software*, vol. 22, no. 10, pp. 1509 – 1518, 2007, modelling, computer-assisted simulations, and mapping of dangerous phenomena for hazard assessment.
- [5] B. Iooss and P. Lemaitre, "A review on global sensitivity analysis methods," in *Uncertainty Management in Simulation-Optimization of Complex Systems*, ser. Operations Research/Computer Science Interfaces Series, 2015, vol. 59, pp. 101–122.
- [6] W. Barreiros, G. Teodoro, T. Kurc, J. Kong, A. C. M. A. Melo, and J. Saltz, "Parallel and Efficient Sensitivity Analysis of Microscopy Image Segmentation Workflows in Hybrid Systems," in *2017 IEEE International Conference on Cluster Computing (CLUSTER)*, Sep. 2017, pp. 25–35.
- [7] G. Teodoro, T. Kurc, L. F. R. Taveira, A. C. M. A. Melo, Y. Gao, J. Kong, and J. Saltz, "Algorithm sensitivity analysis and parameter tuning for tissue image segmentation pipelines," *Bioinformatics*, 2017.
- [8] G. Teodoro, T. Pan, T. Kurc, J. Kong, L. Cooper, S. Klasky, and J. Saltz, "Region templates: Data representation and management for high-throughput image analysis," *Parallel Computing*, vol. 40, no. 10, pp. 589 – 610, 2014.
- [9] J. Kong, L. A. D. Cooper, F. Wang, J. Gao, G. Teodoro, T. Mikkelsen, M. J. Schniederjan, C. S. Moreno, J. H. Saltz, and D. J. Brat, "Machine-based morphologic analysis of glioblastoma using whole-slide pathology images uncovers clinically relevant molecular correlates," *PLoS ONE*, 2013.
- [10] G. Teodoro, T. Pan, T. M. Kurc, J. Kong, L. A. Cooper, N. Podhorszki, S. Klasky, and J. H. Saltz, "High-throughput Analysis of Large Microscopy Image Datasets on CPU-GPU Cluster Platforms," in *27th IEEE International Symposium on Parallel and Distributed Processing (IPDPS)*, 2013.
- [11] G. Teodoro, T. M. Kurc, T. Pan, L. A. Cooper, J. Kong, P. Widener, and J. H. Saltz, "Accelerating Large Scale Image Analyses on Parallel, CPU-GPU Equipped Systems," in *26th IEEE International Parallel and Distributed Processing Symposium (IPDPS)*, 2012, pp. 1093–1104.
- [12] G. Teodoro, R. Sachetto, O. Sertel, M. Gurcan, W. M. Jr., U. Catalyurek, and R. Ferreira, "Coordinating the Use of GPU and CPU for Improving Performance of Compute Intensive Applications," in *IEEE Cluster*, 2009, pp. 1–10.
- [13] G. Teodoro, T. Kurc, G. Andrade, J. Kong, R. Ferreira, and J. Saltz, "Application performance analysis and efficient execution on systems with multi-core cpus, gpus and mics: a case study with microscopy image analysis," *The International Journal of High Performance Computing Applications*, vol. 31, no. 1, pp. 32–51, 2017.
- [14] W. J. C. M. D. McKay, R. J. Beckman, "A Comparison of Three Methods for Selecting Values of Input Variables in the Analysis of Output from a Computer Code," *Technometrics*, vol. 21, no. 2, pp. 239–245, 1979.
- [15] A. Sodani and G. Sohi, "Dynamic instruction reuse," *Proc. Int. Symp. Computer Architecture*, pp. 194–205, 1998.
- [16] B. Mood, D. Gupta, K. Butler, and J. Feigenbaum, "Reuse It Or Lose It: More Efficient Secure Computation Through Reuse of Encrypted Values," *Proceedings of the 2014 ACM SIGSAC Conference on Computer and Communications Security*, pp. Pages 582–596, 2014.
- [17] J. T. J. Goecks, A. Nekrutenko, "Galaxy: a comprehensive approach for supporting accessible, reproducible, and transparent computational research in the life sciences," *Genome Biol.*, vol. 11, no. 8, 2010.
- [18] E. S. Jr. and E. E. Santos, "Effective computational reuse for energy evaluations in protein folding," *International Journal on Artificial Intelligence Tools*, vol. 15, no. 5, pp. 725–739, 2006.
- [19] M. Riera, J. Arnau, and A. González, "Computation reuse in dnns by exploiting input similarity," in *Proceedings of the 45th Annual International Symposium on Computer Architecture*, ser. ISCA '18. Piscataway, NJ, USA: IEEE Press, 2018, pp. 57–68.
- [20] L. Li, E. R. Sparks, K. G. Jamieson, and A. Talwalkar, "Exploiting Reuse in Pipeline-Aware Hyperparameter Tuning," *CoRR*, vol. abs/1903.05176, 2019.
- [21] W. Wang, A. Raghunathan, and N. Jha, "Profiling Driven Computation Reuse: An Embedded Software Synthesis Technique for Energy and Performance Optimization," *Proceedings. 17th International Conference on VLSI Design*, 2004.